Cranial CT findings in sclerosteosis.

S C Hill, S A Stein, A Dwyer, J Altman, R Dorwart and J Doppman

AJNR Am J Neuroradiol 1986, 7 (3) 505-511
http://www.ajnr.org/content/7/3/505

Cranial CT Findings in Sclerosteosis

Suvimol C. Hill[1]
Stuart A. Stein[2]
Andrew Dwyer[1]
Jeremy Altman[3]
Robert Dorwart[1]
John Doppman[1]

Sclerosteosis or Van Buchem's disease is a rare genetic craniotubular hyperostosis that becomes evident in early childhood and is associated with progressive involvement of the skull. The pathologic changes in the cranium noted on CT are described in three cases. Although the disease is incurable, CT is useful to display the morbid anatomy of the cranium before palliative surgery.

Sclerosteosis is an autosomal recessive disorder characterized by bony overgrowth of the skull and tubular bones. The term was first introduced by Hansen in 1967. Until then, sclerosteosis was thought to be a variant of osteopetrosis. Although the radiographic findings of this rare disorder have been described, high-resolution computed tomographic (CT) findings have not. This paper discusses the CT findings in three patients with this disease and correlates them with the clinical and pathologic findings.

Materials and Methods

Three patients were evaluated with routine skull radiographs and CT of the head. CT was performed with a GE-8800 CT/T scanner. Axial 1-cm slices were obtained from the base to the vertex of the skull. The temporal bones and base of the skull were examined in axial and coronal projections at 1.5 mm intervals by using a slice thickness of 1.5 mm. The slices were obtained by using 600 mA, 120 kVp, and a scan time of 9.6 sec. A bone detail algorithm was used to demonstrate the fine bony detail. The area to be examined was targeted, and the images were obtained at 2× or 2.5× magnification by using an extended gray scale of 2000 and an appropriate window level.

The intracranial volumes were estimated by using a cursor to trace an irregular region of interest. The intracranial area of each 1-cm slice from the base of the skull to the vertex was measured, and the areas of all slices were added together to estimate the total intracranial volume. Intracranial volumes of 20 normal patients (14 women, 6 men) ages 6 to 69 years were evaluated in a similar fashion.

Case Reports

Case 1

A 38-year-old man with a history of impaired hearing and bilateral proptosis from the time he was 6 years old was admitted to the NIH for evaluation. The patient also had a history of positional vertigo for 20 years and frontal headaches for 15 years. These symptoms had worsened during the 2 years before the patient was evaluated at the NIH and were accompanied by a loss of memory. On examination, the patient had the facial features of gigantism, with proptosis, asymmetric prognathism, and bilateral facial paralysis and cutaneous syndactyly of the right second and third fingers. Serum calcium and phosphorus were normal; and serum alkaline phosphatase was elevated. The intracranial volume was 876 cm^3. An occipital craniotomy was performed to decompress the posterior cranial fossa, which alleviated the patient's symptoms temporarily. One year later, however, a partial craniectomy

Received May 7, 1985; accepted after revision September 10, 1985.

[1] Diagnostic Radiology Department, The Clinical Center, National Institutes of Health, Bethesda, MD 20205. Address reprints to S. C. Hill, Building 10, Room 1C660.

[2] Department of Neurology, University of Texas Health Sciences, Dallas, TX 75235.

[3] Department of Radiology, Greater Baltimore Medical Center, 6701 N. Charles St., Baltimore, MD 21204.

AJNR 7:505–511, May/June 1986
0195–6108/86/0703–0505

A

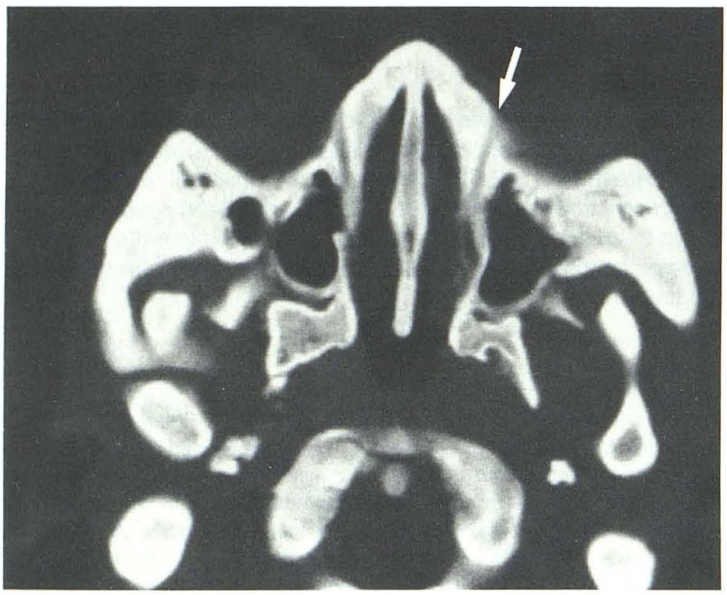

B

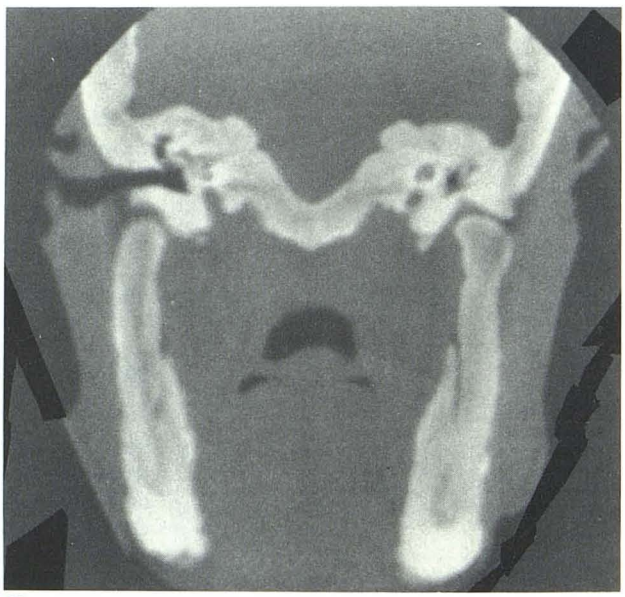

C

Fig. 1.—**A**, Axial CT scan shows diffuse thickening of bony calvarium and obliteration of cerebral sulci and cisterns. **B**, Axial CT scan shows marked thickening of pterygoid plates, maxillary bones, nasal bones, and nasal septum; The mastoid processes are dense and the infraorbital foramina are prominent. There are bilateral long horizontal nasolacrimal ducts (*arrow*). **C**, Coronal CT scan through petrous bones shows diffuse thickening of petrous bones with narrowed internal auditory canals. Note wavy appearance of thickened mandible bilaterally.

was performed because of recurrence of increased intracranial pressure, but the patient died of pneumonia after surgery. An autopsy was obtained.

Case 2

A 48-year-old man (the brother of the patient discussed in Case 1) had a history of bilateral facial paralysis since the age of 7 years and bilateral hearing loss since the age of 10. When the patient was 39 years old, he developed anosmia, followed 6 months later by spontaneous CSF rhinorrhea complicated by meningitis. On examination, the patient showed features of gigantism with bilateral facial paralysis; however, no proptosis or finger syndactyly was present. The serum alkaline phosphatase was elevated. The intracranial volume was 930 cm^3.

Case 3

A 12-year-old black girl had a conductive hearing loss since the age of 3 years and increasing headaches associated with bilateral impaired vision since the age of 10 years. The serum calcium, phosphorus, alkaline phosphatase, and growth hormone were normal. On examination, clinical signs of gigantism, proptosis, and prognathism were present. There was bilateral facial paralysis, bilateral optic atrophy with decreased vision, and cutaneous syndactyly of the left second, third, and fourth fingers. The intracranial volume was 1078 cm^3 and 1050 cm^3 on measurements made 1 year apart. A right jugular venogram demonstrated an outflow obstruction at the level of the right jugular foramen. The right jugular foramen and right facial canals were surgically decompressed. However, the patient's symptoms persisted, and a posterior fossa decompression was performed.

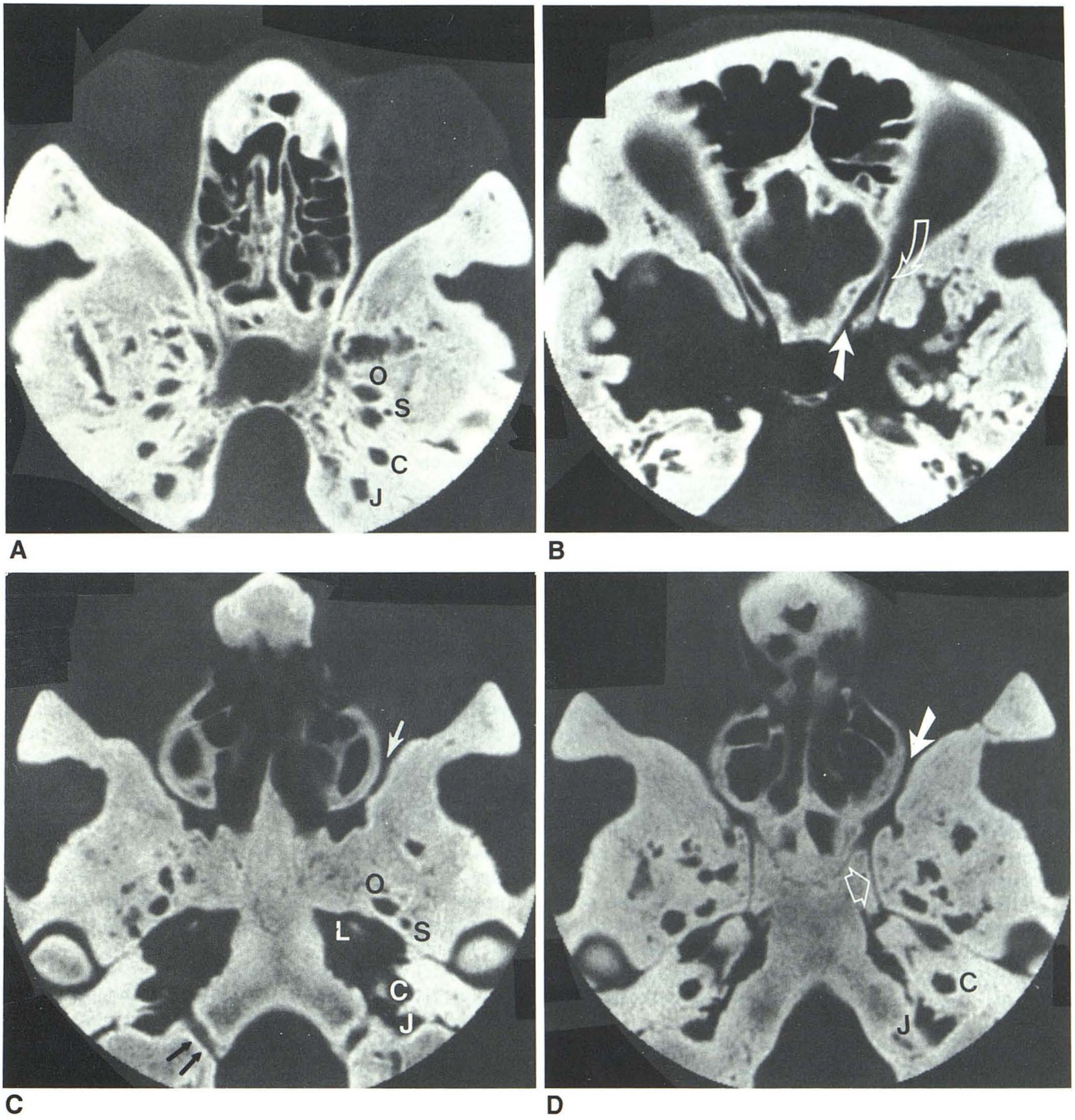

Fig. 2.—**A**, Axial CT scan shows thickening of orbital walls and small orbital volume with bilateral proptosis. Ethmoid sinuses are well aerated but walls are thickened. O = foramen ovale, S = spinosum, C = carotid canal, and J = jugular canal. Several pseudoforamina are formed by bony excrescences. **B**, Axial CT scan shows marked thickening of greater wings of sphenoid bones contributing to narrowing of superior orbital fissures (*open arrow*) that are lateral to optic strut. Optic canals (*arrow*) are also narrowed and elongated. Cranial fossae are small owing to bony excrescences. **C** and **D**; Axial CT scans show narrowed inferior orbital fissures (*white arrow*) and hypoglossal canal (*black arrows*). O, S, C, and J as in 2A. L = lacerum and *open arrow* shows vidian canal.

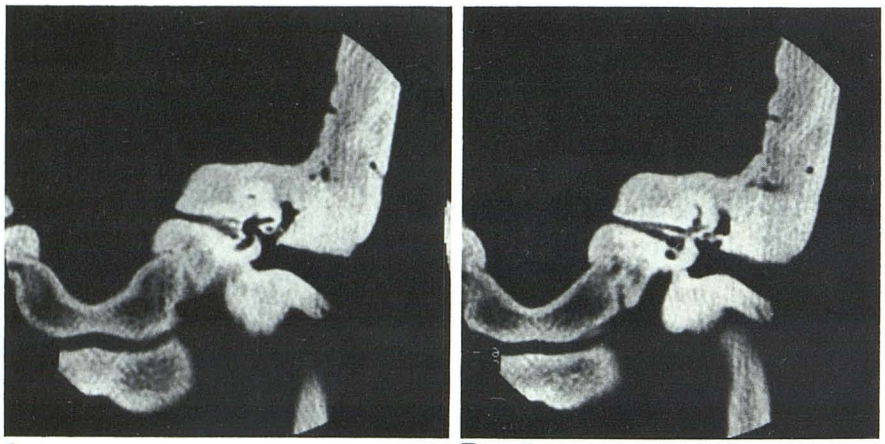

Fig. 3.—**A**, Coronal CT scan at internal auditory canal and vestibule. Horizontal portion of postgeniculate portion of the seventh nerve, which is not normally seen, is walled in as shown. Marked narrowing of internal auditory canal and small epitympanum. **B**, coronal CT scan at level of crista falciformis, which is long and thickened. Facial nerve canal (above) and eighth nerve canal (below). Marked narrowing of internal auditory canal. Ossicles are fused, and incus is fused to lateral wall of epitympanum.

CT Findings

All three cases revealed diffuse thickening of the skull with endocranial excrescences and obliteration of the diploic spaces. The external skull circumferences were in the 95th percentile. The intracranial volumes were smaller than normal. All were within the lowest 10th percentile compared with our normals, which range from 1116 to 1454 cm^3 (average 1255 cm^3; standard deviation, 91.76 cm^3.) (There is a 99% assurance level when the distribution-free tolerance limits of J. W. Tukey are used [1].) There was generalized compression of the brain with obliteration of the cisterns and cerebral sulci (Fig. 1A). In each case, the base of the skull was diffusely thickened with encroachment on several neural foramina. The facial bones, including the nasal bones and the mandible, were thickened (Fig. 1B, C). The paranasal sinuses were normally aerated, but had thickened walls (Fig. 1B). The infraorbital foramina were prominent and the anterior clinoid processes were thickened.

The volumes of the orbits appeared decreased because of thickening of the walls, especially on the lateral sides, and bilateral proptosis and hypertelorism were present (Fig. 2A). The superior and inferior orbital fissures and the optic canals were small (Fig. 2B). The vidian canals were well seen (Fig. 2D).

The petrous bones were markedly thickened with decreased pneumatization of the mastoid air cells interpetrous distance (Fig. 1C and 2B). The external and internal auditory canals were small, as were the epitympanum, hypotympanum, and mesotympanum, but the cochlea, including the semicircular canals and vestibules, were normal. There was distortion and fusion of the ossicles (Fig. 3) in two patients. The vestibular aqueducts were not identified and the cochlea aqueducts were small. The seventh nerve canals were small throughout their entire courses (Fig. 4A). Both oval and round windows were severely narrowed (Fig. 4B). The carotid and jugular canals were small (Figs. 2C, 5A, and 5B) and the latter had an abnormal configuration. Venous collateral circulation was also seen (Fig. 5B). The cranial CT findings are listed in Tables 1 and 2.

Discussion

In 1967, Hansen [2] first introduced the term "sclerosteosis" to describe a familial disorder associated with generalized osteosclerosis and characterized by a thickening of the bony calvaria and facial bones, as well as syndactyly of the digits. This condition was previously mistaken as a variant of osteopetrosis. Van Buchem in Holland reported two cases of hyperostosis corticalis generalizata familiaris in 1955 [3]. He later found 15 additional cases and renamed the condition Van Buchem's disease. The reason for classifying Van Buchem's disease as separate from sclerosteosis is unclear because there is no substantial difference between the cases described by Van Buchem and 25 South African sclerosteosis patients described by Beighton and Hamersma in 1976 [4]. In fact, we believe they are the same disease. The slight difference in the clinical picture between Van Buchem's disease and sclerosteosis is simply due to variability in the disease's manifestations. The incidence is increased with inbreeding. An autosomal recessive inheritance has been suggested [5], but the exact genetic basis of the disease is still unclear.

Until now, approximately 60 cases of sclerosteosis, including Van Buchem's disease, have been reported in the literature. The exact etiology is not known. Analysis of bone kinetics, however, has demonstrated increased osteoblastic activity associated with elevation of serum alkaline phosphatase. Bone overgrowth may be due to osteoblastic hyperactivity rather than to decreased osteoclastic activity (6).

The age of onset of the clinical symptoms is usually early childhood, sometimes as young as 2 years. Patients usually present with facial nerve palsies, hearing loss, or serous otitis. They are usually physically large, many in the 98th percentile, and their growth rates are accelerated. Headaches accompanied by visual problems and symptoms of other cranial nerve involvement can develop in later childhood. Eventually patients develop increased intracranial pressure or become blind and commonly die in their thirties.

Clinically, the diagnosis is suggested by the presence of specific facial dysmorphism (prognathism, frontal bossing,

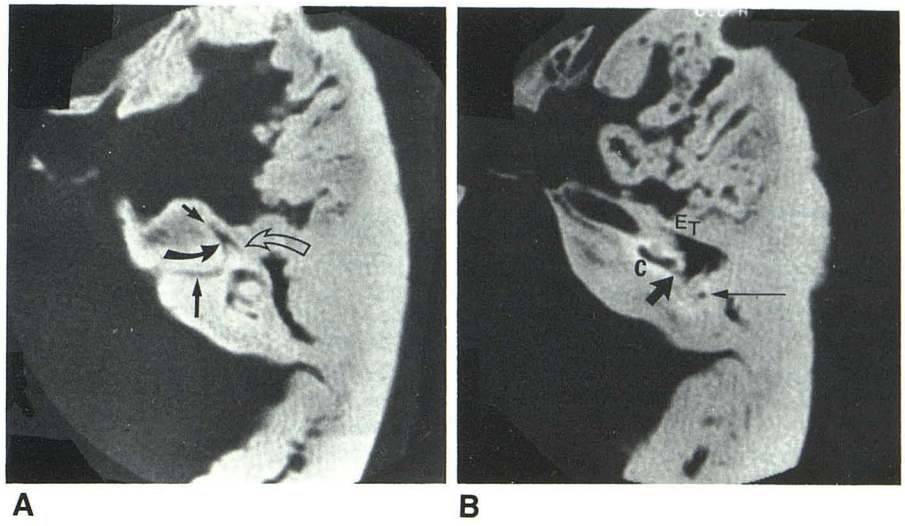

Fig. 4.—**A**, Axial CT scan through upper internal auditory canal and vestibule, which shows facial nerve canal (*straight arrow*) coming up to geniculate ganglion (*curved arrows*) as well as takeoff of greater superficial petrosal nerve (*short arrow*). **B**, Axial CT scan at level of basal turn of cochlea (C) and round window (*thick arrow*); vertical portion of seventh nerve (*long arrow*) and the eustachian tube (ET).

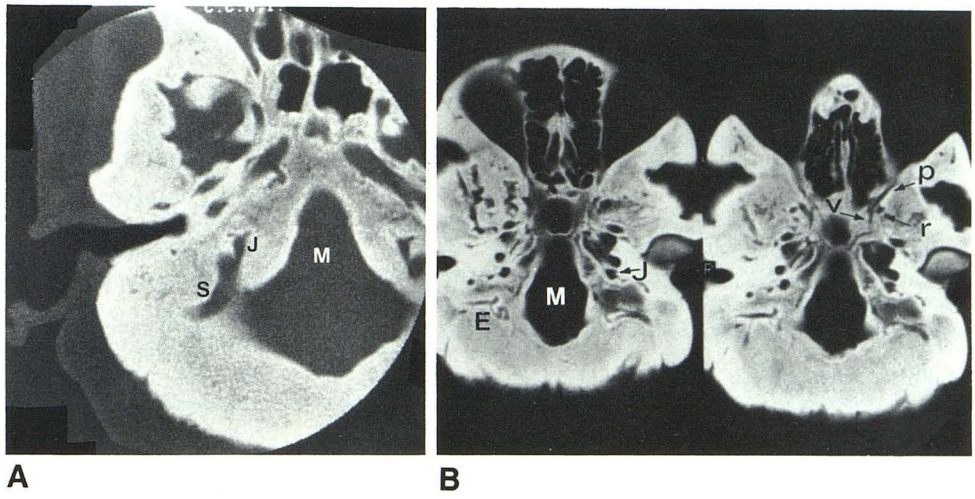

Fig. 5.—**A**, Axial CT scan shows small foramen magnum (M) with overgrowth of basiocciput and exocciput on each side resulting in narrowing of space for brain stem. Jugular bulb (J) is small with prominent groove of sigmoid sinus (S). **B**, Axial CT scans through skull base show small foramen magnum (M) and jugular canals (J) with evidence of venous collateral channels or emissary veins (E). Anterior portion of the vidian canal (V) with foramen rotundum (r) as well as pterygomaxillary fissure (p).

proptosis, ocular hypertelorism), accelerated growth, and cranial nerve palsies, with or without finger syndactyly.

Similar cranial nerve complications are found in other disorders, including osteogenesis imperfecta, Paget's disease, fibrous dysplasia, osteopetrosis (Albers-Schonberg's disease), genetic craniotubular dysplasia, and genetic craniotubular dysostoses [6–11]. These diseases are differentiated [12] on the basis of the pattern of inheritance, age of manifestation, changes in the long bones, presence or absence of spinal involvement, and associated clinical manifestations and laboratory findings. They all have varying degrees of thickening of the cranial vault and skull base.

In osteosclerosis, which includes osteopetrosis and pycnodysostosis, the prominent feature is increased bone density. In contrast to sclerosteosis, pycnodysostosis is a form of shortlimb dwarfism with a small mandible, hypoplasia of distal clavicles, and distal phalangeal aplasia of fingers and toes. In malignant recessive osteopetrosis, the obvious clinical distinctions are dwarfism, anemia, hypocalcemia, pathologic fractures, and mental retardation.

There is loss of corticomedullary distinction of bones in osteopetrosis with involvement of the epiphyses, metaphyses, and diaphyses as opposed to the diaphyseal involvement seen in sclerosteosis.

The main feature of genetic craniotubular dysplasia is abnormal modeling of the tubular bones. This group includes craniometaphyseal dysplasia, craniodiaphyseal dysplasia, frontometaphyseal dysplasia, and dysosteosclerosis. The differences are in the distribution of the bone sclerosis. Cranial and facial hyperostosis and sclerosis are more severe in craniodiaphyseal dysplasia than in sclerosteosis and progress more rapidly without cortical thickening of the tubular bones. In dysosteosclerosis there is flattening, dorsal wedging, and sclerosis of the vertebral bodies with wide metaphyseal flare and increased bone fragility as well as dental anomalies.

Overgrowth of the cranium and tubular bones are the main features in the genetic craniotubular hyperostoses, Van Buchem's disease (or sclerosteosis), congenital hyperphosphatasia, and progressive diaphyseal dysplasia. However, in congenital hyperphosphatasia, the patient is dwarfed and there

TABLE 1: **Cranial CT Findings in Three Patients with Sclerosteosis**

	Case 1	Case 2	Case 3
Calvarium			
Ant. cranial fossa	Diffusely thickened with obliteration of diploic spaces and endocranial bony excrescences; small cranial fossae	Same	Same
Middle cranial fossa			
Postcranial fossa			
Brain	General compression with obliteration of cisterns; absent sulci	Same	Same
Lateral ventricles	Mildly dilated status post placement of epidural pressure-monitoring device	Mildly reduced	Mildly dilated status postplacement of epidural pressure-monitoring device
Facial bones			
Nasal bones	Thickened	Same	Same
Sinuses	Well developed with thickened walls	Same	Same
Nasolacrimal ducts	Nearly horizontal, short, narrow	Not studied	Not studied
Orbits			
Volumes	Decreased, with proptosis	Same	Same
Wall thickening	Mostly lateral	Same	Same
Hypertelorism	Present	Same	Same
Infraorbital foramen	Prominent	Not studied	Not studied
Superior orbital fissure	Narrowed	Same	Same
Inferior orbital fissure	Narrowed	Narrowed with excrescence	Severely narrowed
Optic canals	Small	Mildly compromised	Not studied
Ant. clinoid processes	Short and fat	Thickened	Same
Base of skull			
Foramen magnum	Small	Normal	Small
Interpetrous distance	Decreased	Same	Same
Sphenoid sinus	Nonaerated	Thickened wall; partially aerated	Small
Foramina			
Ovale	Probably small	Small, R > L	Not studied
Rotundum	Oblique, vertical course	Elongated	Normal
Spinosum	Normal	R enlarged; L small	Not studied
Vidian canal (pterygoid)	Normal	Normal, well seen	Normal
Ant. condylar canal (hypoglossal)	Normal	Mildly narrowed bilaterally	R obliterated
Post condylar canal (hypoglossal)	Present, with prominent emissary vein	Same	Not seen; many emissary veins in middle cranial fossa
Lacerum	Normal	Normal	Normal
Petros bones			
Mastoid aeration	Markedly decreased, bilaterally	Same	Same
Carotid canal	Small	Small	Small
Jugular foramen	Small, abnormal configuration	Very small, bilaterally	Operated and small on R; very small on L
External auditory canal	Small	Small	Small
Mesotympanum	Small	Small	Distorted on R side; small on L
Hypotympanum	Small, narrowed eustachian tube	Same	Same
Epitympanum (ossicles)	Fused R, L deformed	Normal	Distorted; surgery R; L fused
Cochlea	Normal	Normal	Normal
Vestibule	Normal	Normal	Normal
Semicircular canals	Normal	Normal	Normal
Vestibular aqueducts	Not identified R and L	Not identified	Not identified
Cochlea aqueducts	Normal R and L	Small R and L	Not studied; not seen
IAC with cochlea and vestibule	Small	Small bilaterally	Narrow bilaterally
VII nerve anatomy labyrinthine canal (pregeniculate)	Small	Small	Slightly prominent
Greater superficial petrosal nerve canal	Prominent	Small	Not identified
Postgeniculate segment			
Horizontal	Small	Small	Normal R, small L
Vertical	Small	Small	Normal R; small L
Stylo mastoid foramen	Abn. configuration small R and L	Small	Normal R, small L
Oval window	Occluded R, severely stenosed	Small bilaterally	Small
Round window	Severely stenosed	Small bilaterally	Severely stenosed

Note. Ant. = anterior, R = right, L = left.

TABLE 2: **Correlation of Clinical Symptoms and CT Findings in Three Patients***

Abnormal Cranial Nerve Function	Foramen	No. of Patients with Symptoms / No. of Patients with Abnormal CT
CN II†	Optic canal	2/2
CN V	Foramen ovale	2/2
CN VII & VIII	Internal auditory canal	3/3
CN IX & X	Jugular foramen	3/3
CN XII‡	Hypoglossal canal	1/3

* All 3 patients have hyposmia but we are unable to evaluate the cribiform plates.
† 100% correlation in CN II, V, VII, VIII, IX, and X.
‡ Imperfect correlation of CN XII.

is increased bone fragility. The cortical bone is replaced by trabecular bone. In progressive diaphyseal dysplasia, there is mild cranial sclerosis with neuromuscular dysfunction. Finally, the clinical appearance of acromegalic patients may mimic sclerosteosis, but radiographically the thickening and sclerosis of the skull and facial bones are less prominent, without diaphyseal thickening of tubular bones, and there is erosion or enlargement of the sella turcica.

Before the advent of CT, sclerosteosis had been described extensively (4, 8, 13, 14), but CT allows a more accurate and complete demonstration of the morbid anatomy [15].

The disease remains an incurable and potentially lethal process of inexorable bony encroachment on the cranial cavity and foramina. CT, by virtue of excellent anatomic display, provides a better basis for decisions regarding surgical intervention and for studies of the disease chronology and response to therapy. Cranial thickening and resulting compressive effects on the sulci, cisterns, and brain are evident. Regarding cranial nerve involvement, there were several problems in interpreting the CT studies because of normal variations in the size of the cranial nerve foramina. Nevertheless, there was good correlation between the foraminal narrowing noted by CT and clinical involvement of the cranial nerves, except for the hypoglossal canal (Table 2). This may be explained by difficulty in evaluation of the function of the hypoglossal nerve and geometric problems in evaluating a small canal whose axis is the same plane as the slice. There is also difficulty in distinguishing the true foramina from pseudoforamina formed by the bone excrescences, especially in the skull base.

One of the most common clinical problems in patients with sclerosteosis is conductive and nerve deafness. Fusion of the ossicles was well demonstrated by CT as was the marked narrowing of the internal auditory canals, oval windows, round windows, and vestibular and cochlear aqueducts.

REFERENCES

1. Diem K, ed. *Documenta Geigy: Scientific tables.* Ardsley, New York: Geigy Pharmaceuticals, **1962**:128
2. Beighton P, Cremin BJ, Hamersma H. The radiology of sclerosteosis. *Br J Radiol* **1976**;49:934–939
3. Van Buchem FSP, Hadders HN, Hansen JF, Woldring MG. Hyperostosis corticalis generalisata—a report of seven cases. *Am J Med* **1962**;33:387–397
4. Beighton P, Hamersma H. Sclerosteosis in South Africa. *S Afr Med J* **1979**;55:783–788
5. Gorlin RJ, Spranger J, Koszalka MF. Genetic craniotubular bone dysplasias and hyperostoses: a critical analysis. *Birth Defects: Original Article Series.* April **1969**; V,(4)
6. Stein SA, Witkop C, Hill S, et al. Sclerosteosis: neurogenetic and pathophysiologic analysis of an American kinship. *Neurology* **1983**;33:267–277
7. Suga F, Lindsay JR. Temporal bone histopathology of osteopetrosis. *Ann Otol* **1976**;85:15–24
8. Van Buchem FSP, Prick JJG, Jaspar HHJ. Hyperostosis corticalis generalisata familiaris (Van Buchem's disease). New York: American Elsevier, **1976**
9. Hamersma H. Facial nerve paralysis in the osteopetrosis. In: Fisch U, ed. *Facial nerve surgery.* Amstelveen, The Netherlands: Kugler Medical Publications, **1977**:555–572
10. Lehman RAW, Reeves JD, Wilson WB, Wesenberg RL. Neurological complications of infantile osteopetrosis. *Ann Neurol* **1977**;2:378–384
11. Spranger J, Langer L, Wiedemann HR. *Bone dysplasias: an atlas of constitutional disorders of skeletal development.* Philadelphia: W. B. Saunders, **1974**
12. Sugiura Y, Yasuhara T. Sclerosteosis: a case report. *J Bone and Joint Surg* [Am] March **1975**;57-A(2):273–277
13. Nager GT, Stein SA, Dorst JP, et al. Sclerosteosis involving the temporal bone: clinical and radiologic aspects. *Am J Otolaryngo* **1983**;4:1–17
14. Beighton P, Hamersma H. The clinical features of sclerosteosis: a review of the manifestations in twenty-five affected individuals. *Ann Int Med* **1976**;84:393–397
15. Virapongse C, Rothman SLG, Kier EL, Sarwar M. Computed tomographic anatomy of the temporal bone. *AJNR* **1982**;3:379–389, *AJR* **1982**;139:739–749